Stationary H-Mode Discharges with Internal Transport Barrier on ASDEX Upgrade

O. Gruber, R. C. Wolf, R. Dux, C. Fuchs, S. Günter, A. Kallenbach, K. Lackner, M. Maraschek, P. J. McCarthy,* H. Meister, G. Pereverzev, F. Ryter, J. Schweinzer, U. Seidel, S. Sesnic, A. Stäbler, J. Stober, and the ASDEX Upgrade Team

Max-Planck-Institut für Plasmaphysik, EURATOM-Assocation, D-85748 Garching, Germany

(Received 29 October 1998)

Stationary discharges with H-mode edge and internal transport barrier for energy, momentum, and particle transport have been obtained on ASDEX Upgrade. At a line averaged density of 4×10^{19} m^{-3} an H factor of $H_{\mathrm{ITER89\text{-}P}} = 2.4$ and $\beta_N = 2$ could be maintained for 6 s corresponding to 40 confinement times, limited only by the possible discharge duration. The q profile is flat in the center and close to 1. Current diffusion calculations suggest that reconnection is required to clamp the safety factor at 1, which in the absence of sawteeth is explained by the strong fishbone activity.

PACS numbers: 52.55.Fa, 52.25.Fi

Improved confinement related to the modification of the current profile was observed in several tokamaks. Common to these regimes of operation is the flattening of the central current profile corresponding to a zero or even negative value of the central magnetic shear ($s = \frac{r}{q}\frac{dq}{dr}$, where q is the safety factor). There is increasing evidence that, in addition to magnetic shear stabilization, a combination with $\mathbf{E} \times \mathbf{B}$ shear stabilization is required for the initiation of internal transport barriers (ITB) [1,2].

In most experiments additional heating in the current ramp phase is used to reduce current diffusion and hence generate a broad or hollow current profile with q above 1. TFTR [3], DIII-D [4], and JT60-U [5] achieve this by neutral beam heating (NBI), while JET uses a combination of lower hybrid current drive, ion cyclotron heating, and NBI [6]. Discharges with improved core confinement or ITBs have been established with both L-mode edge like the negative central shear plasmas in DIII-D [7] and ELMy H-mode edge plasma parameters like JET ELMy H-mode discharges with ITB [8], or JT60-U high β_p H-mode discharges [9,10], some of which have been approaching steady state conditions.

On ASDEX Upgrade a stationary regime of operation has been found which shows improved core confinement of both electrons and ions in combination with an H-mode edge. In Fig. 1 the main plasma parameters of such a discharge are illustrated. During the current ramp of 1 MA/s moderate neutral heating of 2.5 MW is applied, to reduce current diffusion. At 1 s the current flat top is reached and the X point is formed. Simultaneously, the NBI power is raised to 5 MW, the L-H transition occurs, and the line averaged density is kept at 4×10^{19} m^{-3}. At a toroidal magnetic field of 2.5 T and a plasma current of 1 MA q_{95} is 4. While during the current ramp at 2.5 MW heating power electron and ion temperatures increase at the same rate; T_i reaches almost twice the value of T_e when the heating power is doubled, as 75% of the power is going into the ions. The high performance phase lasts for 6 s, limited only by the prescribed duration of the NBI. This corresponds to 40 confinement times or $\approx$2.5 resistive time scales for internal current redistribution, which here is the time for a current perturbation to diffuse over half of the minor radius. Current profiles from an equilibrium reconstruction using the multichannel motional Stark effect (MSE) polarimeter [11] confirm that the current profile remains stationary shortly after the full neutral beam power is applied. In addition, the measured loop voltage is also stationary within 10%.

The profiles of plasma temperature, density, and toroidal rotational velocity [Fig. 2(a)] show, in addition to the H-mode pedestal, an increase starting at $\rho_{\mathrm{tor}} = 0.6$,

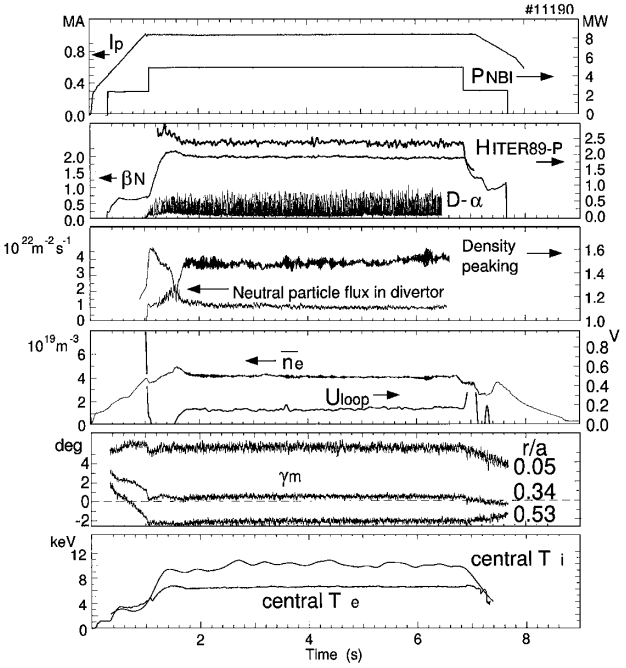

FIG. 1. Time evolution of plasma current (I_p), neutral beam heating power (P_{NBI}), H factor ($H_{\mathrm{ITER89\text{-}P}}$), normalized β (β_N), divertor D_α radiation, density peaking and neutral particle flux in the divertor, line averaged density ($\overline{n}_e$), loop voltage (U_{loop}), MSE polarization angles (γ_m) at three radial locations r/a, and central electron and ion temperatures ($T_{e,i}$) for a stationary discharge with ITB and H-mode edge.

which is attributed to the formation of an ITB. The strong density peaking of $n_{e0}/\overline{n}_e = 1.5$ suggests that not only the energy but also the particle confinement is improved. Compared to ASDEX Upgrade internal transport barriers with L-mode edge at the same power [12], the gradients are less pronounced, while the central v_{tor} is comparable. The central T_i is still more than a factor of 2 above the ELMy H-mode level. For comparison, the profiles of T_i, T_e, n_e, and v_{tor} for a standard ELMy H-mode discharge are plotted in Fig. 2(b), exhibiting lower central values of all quantities (except for the density). This is also reflected in low values of $\beta_N \approx 1.6$ and $H_{\text{ITER89-}P} \approx 1.8$, compared to $\beta_N \approx 2$ and $H_{\text{ITER89-}P} \approx 2.4$ for discharge #11190. The density of the sawtoothing discharge is slightly higher than that of the ITB discharge, as standard H-mode plasmas with sawteeth at lower densities suffer from neoclassical tearing modes, resulting in an even more degraded confinement.

The only MHD activity observed in the core of the plasma is strong $(1,1)$ fishbones which start at 1.1 s and accompany the whole 5 MW heating phase, indicating that the central q is in the vicinity of 1, but not low enough for the formation of sawteeth. The plasma edge is that of an ELMy H mode, as seen on the D_α trace. The fishbone oscillations seem to behave like a resistive MHD instability [13]. Similar to sawteeth, but on a much faster time scale, the soft x-ray (SXR) profiles from a 1D deconvolution of the line integrated SXR emissivities show a relaxation oscillation expelling energy and possibly also impurities. This is confirmed by T_e measurements using electron cyclotron emission. The fishbones change the temperature of the background plasma on a much faster time scale ($\approx$1 ms) than would follow from the redistribution of the fast particles, and consequently of the heating power. The magnetic reconnection due to fishbones would also explain that sawteeth do not appear, as the fishbone oscillations could serve as a mechanism for keeping q at 1. When increasing the beam power, β_N was limited by the occurrence of $(3,2)$ neoclassical tearing modes, the onset of which was always preceded by a fishbone. Because of the low density, the $(3,2)$ modes were usually followed by $(2,1)$ modes which ultimately lock. Considering that sawteeth are not present, the second harmonic of a $(1,1)$ fishbone acts as a seed island for the initiation of $(3,2)$ neoclassical tearing modes [14]. The β limit is close to $\beta_N = 2.2$. At 6.25 MW of NBI $\beta_N = 2.2$ still could be maintained for a duration of 1 s after which, due to the proximity of the β limit, a $(3,2)$ mode occurred.

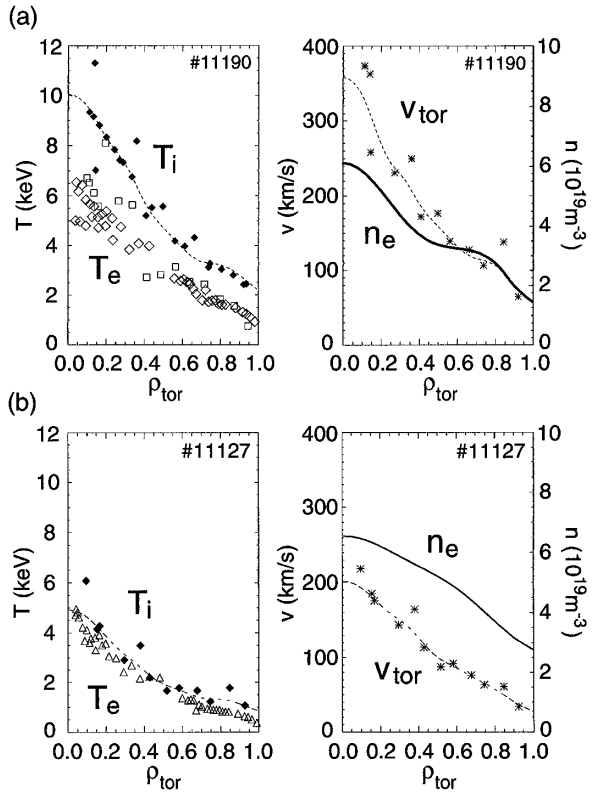

FIG. 2. (a) Radial profiles of ion and electron temperatures [◇: electron cyclotron emission (ECE); □: Thomson scattering], electron density, toroidal rotational velocity (v_{tor}) of the discharge presented in Fig. 1 (#11190). The profiles are quasistationary during the 5 MW heating phase. (b) For comparison, the profiles of a sawtoothing discharge with the same heating power and comparable density are plotted (T_e from ECE only).

For the sustainment of the ITB the heating power during the current ramp is very critical. Applying more NBI power during the current ramp resulted in large scale MHD instability as soon as the L-H transition occurred. Discharges without preheating in the current ramp show only a transient improvement of the plasma confinement indicating that the current profile so obtained cannot stabilize the larger pressure gradients. A $(3,2)$ neoclassical tearing mode leads to a deterioration of the confinement and finally to $(2,1)$ locked modes.

A major concern regarding the stationary plasma operation with improved confinement is the behavior of the impurity content. From spectroscopic data the main impurities have been identified as helium (5%), carbon (2.5%), oxygen (1.2%), and silicon (0.3%) after siliconization of the vacuum vessel [15]. Charge exchange recombination spectroscopy yields a flat concentration profile of carbon, and the 1D deconvolution of SXR measurements indicates no temporal accumulation of impurities in the center. Neglecting the presence of elements with Z larger than Si, an upper limit of Z_{eff} can be inferred from SXR emissivities by using the impurity transport code STRAHL [16]. The calculation assumes flat profiles for the concentration of He, C, and O and fits the Si profile to the measured SXR emissivity. The resulting Z_{eff} profile is slightly peaked in the center (see Fig. 3) and quasistationary from 2 s until the end of the 5 MW heating phase. The peaking of the electron density is partially caused by the impurities, but nevertheless, also the deuteron density is increasing towards the plasma center. The stationarity is possibly caused by the strong fishbone

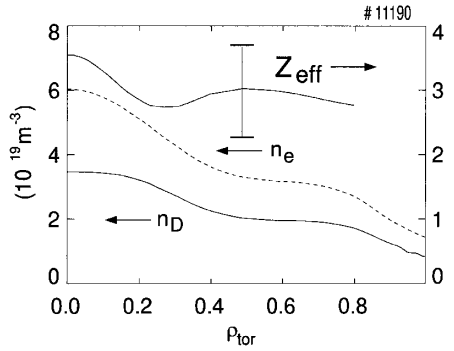

FIG. 3. Radial profiles of electron, deuteron density (n_D), and Z_{eff} at 4 s of discharge #11190. n_e is based on DCN laser interferometer and lithium beam measurements. From this and the various impurity concentrations n_D is inferred.

activity expelling, similar to sawteeth, impurities from the plasma core.

Energy transport has been analyzed using the $1\frac{1}{2}$-D ASTRA code. Besides electron density, ion and electron temperature profiles, profiles of the radiated power and Z_{eff} have been incorporated in the study. In Fig. 4 the resulting ion and electron thermal conductivities are shown. In the central regions of the plasma χ_i drops to neoclassical values, but also χ_e is at a low level indicating that the transport reduction is not limited to the ions.

The q profile inferred from MSE, which is illustrated in Fig. 5(a), shows an extended low shear region in the plasma center with $q_0 \approx 1$ and remains stationary throughout the discharge, which is exemplified by the time traces of q_0, $q_{\min}$, and the radius of the $(1, 1)$ surface in Fig. 5(b) and is consistent with the fixed location of the $(1, 1)$ fishbone mode derived from the SXR. To reproduce this behavior in an ASTRA simulation, which solves the current diffusion equation using the experimental temperature and Z_{eff} evolution, Kadomtsev reconnection [17] has to be invoked, which redistributes the central current as soon as q drops below 1. Without this reconnection mechanism the calculated q_0 drops towards 0.7, which is inconsistent with the MSE result. As no sawteeth have been observed,

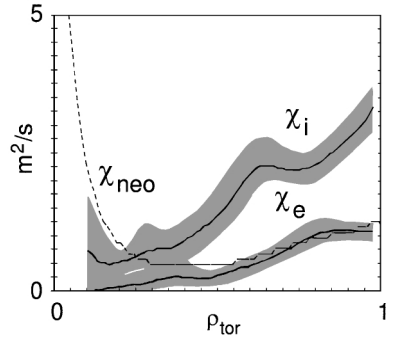

FIG. 4. Ion and electron thermal conductivity at 2.5 s of discharge #11190 vs normalized toroidal flux. Also shown is the neoclassical ion thermal conductivity [18].

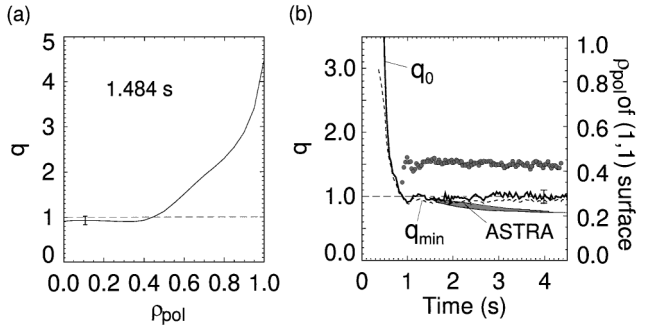

FIG. 5. Safety factor profile (a) and time traces of q_0 and $q_{\min}$ (b) inferred from MSE of a stationary discharge with ITB. Also shown is the calculated evolution of q_0 using neoclassical current diffusion (ASTRA code) without reconnection. As the initial condition the current density profile from MSE at 1.484 s has been used. The shaded area represents the uncertainty due to variations of T_e by $\pm 15\%$, which is a conservative estimate of the error of the ECE measurements, and Z_{eff} between 1 and the profile shown in Fig. 3.

the reconnection, required to explain the clamping of the central q, is attributed to the strong $(1, 1)$ fishbone activity. The total current, the composition of which is derived from ASTRA, consists of 70% Ohmic current, 10% current drive from NBI, and 20% bootstrap current, the small bootstrap current fraction corresponding to relatively moderate values of β_N and q_{95}.

Both raising the density and reducing the heating power resulted in a deterioration of the confinement, which is accompanied by the appearance of sawtooth oscillations when T_i approaches T_e. A discharge, where the line averaged density was increased from 4.2×10^{19} to

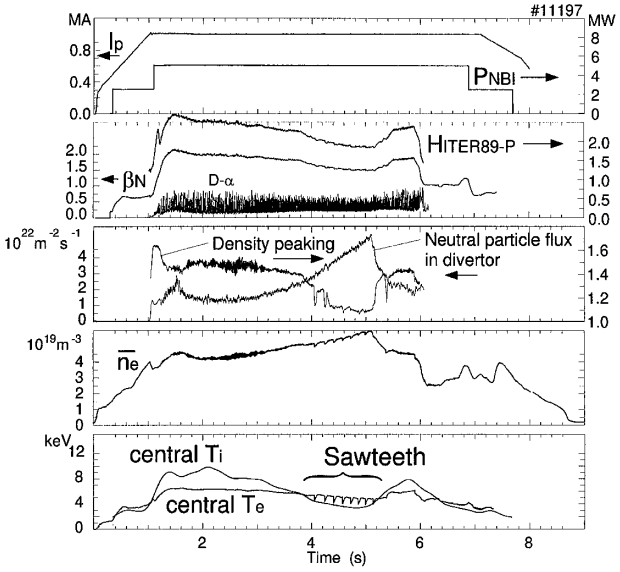

FIG. 6. I_p, P_{NBI}, H factor, β_N, D_α signal, density peaking factor, neutral particle flux in the divertor, line averaged density, and central temperatures of a discharge where after the formation of the ITB the density was increased.

5.8×10^{19} m^{-3} is shown in Fig. 6. Associated with the increase of the density was an increase of the neutral particle flux in the divertor, representing the particle source for the main plasma, and a simultaneous reduction of the density peaking. The central ion temperature and the toroidal rotation velocity decreased by more than a factor of 2. On T_e the effect is less prominent, as with the drop if T_i more power is going into the electrons. Also the amplitude of the fishbone oscillations decreases. It is seen from the β_N and $H_{\mathrm{ITER89\text{-}}P}$ traces that the confinement drops, which means, as the power is kept constant, the temperature decrease is stronger than the corresponding density increase. It is interesting to note that, after decreasing the density again, the ITB recovers partially, although it is finally terminated by a $(3, 2)$ mode. This suggests that the stability of the regime could not be recovered entirely. The influence of the neutral particle flux has also been observed in cases where the cryopump, which has been used in the discharges described so far, has not been in operation. After increasing the NBI power to 5 MW an ITB is formed transiently lasting only 100 ms. While the density is 15% higher than in the cases where the ITB could be sustained, the neutral particle flux is about a factor of 3 higher.

In summary, stationary internal transport barriers combined with an H-mode edge barrier have been produced, which last for 40 confinement or more than 2 current diffusion times. $\beta_N = 2$ and a high H factor result in a stationary value of $\beta_N \times H_{\mathrm{ITER89\text{-}}P} = 4.8$. The discharges show the highest $n_{D,0} T_{i,0} \tau_E$ so far observed on ASDEX Upgrade. 7×10^{19} keV s m^{-3} have been maintained for 6 s and 7.5×10^{19} keV s m^{-3} for 1 s. The stationarity of the discharges is associated with a fishbone induced stabilization of the current profile occurring with small scale perturbations, which in contrast to sawteeth are compatible with improved confinement. β is limited by the occurrence of neoclassical tearing modes which are initiated by fishbones.

The authors would like to thank B. Rice and T. Taylor from DIII-D for fruitful discussions.

*Permanent address: University College Cork, Association EURATOM-DCU, Cork, Ireland.

[1] K. H. Burell, Phys. Plasmas **4**, 1499 (1997).
[2] E. Synakowski, Plasma Phys. Controlled Fusion **40**, 581 (1998).
[3] F. M. Levinton *et al.*, Phys. Rev. Lett. **75**, 4417 (1995).
[4] E. J. Strait *et al.*, Phys. Rev. Lett. **75**, 4421 (1995).
[5] T. Fujita *et al.*, in *Proceedings of the 16th International Conference on Plasma Physics and Controlled Fusion Research, Montreal, 1996* (Report No. IAEA-CN-60/A3-I2, 1996).
[6] A. C. C. Sips *et al.*, Plasma Phys. Controlled Fusion **40**, 1171 (1998).
[7] B. W. Rice *et al.*, Phys. Plasmas **3**, 1983 (1996).
[8] F. X. Söldner *et al.*, Plasma Phys. Controlled Fusion **39**, B353 (1997).
[9] T. Fujita *et al.*, Plasma Phys. Controlled Fusion **39**, B75 (1997).
[10] Y. Kamada *et al.*, in *Proceedings of the 17th International Conference on Plasma Physics and Controlled Fusion Research, Yokohama, 1998* (Report No. IAEA-F1-CN-69/CD2/EX9/2).
[11] R. C. Wolf *et al.*, in *Proceedings of the 24th European Conference on Controlled Fusion and Plasma Physics, Berchtesgaden, 1997* (EPS, Geneva, 1997), Pt. IV, p. 1509.
[12] G. Pereverzev *et al.*, in *Proceedings of the 25th European Conference on Controlled Fusion and Plasma Physics, Prague, 1998* (EPS, Geneva, 1998).
[13] S. Günter *et al.*, Nucl. Fusion **38**, 1431 (1998).
[14] A. Gude *et al.*, Nucl. Fusion **39**, 127 (1999).
[15] J. Winter *et al.*, Phys. Rev. Lett. **71**, 1549 (1993).
[16] K. Behringer, JET Report No. JET-R(87)08, 1987.
[17] B. B. Kadomtsev, Sov. J. Plasma Phys. **75**, 389 (1975).
[18] C. S. Chang and F. L. Hinton, Phys. Fluids **29**, 3314 (1986).